

# Microsatellite Instability and Gene Mutations in Transforming Growth Factor-Beta Type II receptor Are Absent in Small Bowel Carcinoid Tumors

Mark Kidd, Ph.D.<sup>1</sup>  
 Geeta Eick, Ph.D.<sup>1</sup>  
 Michael D. Shapiro, B.S.<sup>1</sup>  
 Robert L. Camp, M.D., Ph.D.<sup>2</sup>  
 Shrikant M. Mane, Ph.D.<sup>3</sup>  
 Irvin M. Modlin, M.D., Ph.D.<sup>1</sup>

<sup>1</sup> Department of Surgery, Yale University School of Medicine, New Haven, Connecticut.

<sup>2</sup> Department of Pathology, Yale University School of Medicine, New Haven, Connecticut.

<sup>3</sup> Howard Hughes Medical Institute (HHMI) Keck Institute, Yale University School of Medicine, New Haven, Connecticut.

Dr. Kidd and Dr. Eick contributed equally to the current article.

Address for reprints: Mark Kidd, Ph.D., Department of Surgery, Yale University School of Medicine, 333 Cedar Street, P.O. Box 208062, New Haven, CT 06520-8062; Fax: (203) 737-4067; E-mail: mkidd01@snet.net

Received May 31, 2004; revision received September 20, 2004; accepted September 20, 2004.

**BACKGROUND.** Microsatellite instability (MSI) with concomitant mutations in the coding region of transforming growth factor-beta type II receptor (TGF $\beta$ RII) results in an aberrant growth-regulatory phenotype in colorectal carcinomas. The authors postulated that a similar mechanism occurred during the malignant evolution of small bowel carcinoid tumors.

**METHODS.** Mutational analysis of two coding regions in the TGF $\beta$ RII gene associated with MSI and BAT-26 within intron 5 of the mismatch repair gene, *hMSH2*, was undertaken in small bowel carcinoids ( $n = 14$ ), lymph node metastasis ( $n = 1$ ) and liver metastases ( $n = 5$ ). Quantitative PCR analysis (TAQMAN, Applied Biosystems, Foster City, CA) was then undertaken to examine gene alterations in mismatch repair genes (*hMLH1* and *hMSH2*) in small bowel carcinoids ( $n = 7$ ) and matched normal mucosa ( $n = 5$ ). Staining was then analyzed using quantitative tissue array profiling (AQUA analysis) in a small bowel EC carcinoid tissue microarray ( $n = 55$  tumors) with immunostaining against TGF $\beta$ RII and MSH2.

**RESULTS.** Mutational examination of the TGF $\beta$ RII gene and BAT-26 demonstrated that MSI was not present in any carcinoid material. Q RT-PCR analysis demonstrated statistically significant increased message levels of *hMSH2* but not *hMLH1* in carcinoid tumors. Quantitative analysis of membrane TGF $\beta$ RII immunostaining using AQUA demonstrated that TGF $\beta$ RII expression was down-regulated ( $P < 0.0002$ ) in thirty-three primary small bowel carcinoids that exhibited lymph node and liver metastases compared to normal mucosa. AQUA analysis of nuclear MSH2 immunostaining demonstrated no differences for MSH2 between normal tissue and carcinoid tumor metastasis. Small bowel carcinoids characterized by variable expression of TGF $\beta$ RII, did not exhibit MSI and had no differences in MSH2 expression.

**CONCLUSIONS.** The molecular events leading to the formation of carcinoid tumors in the small bowel were different from those resulting in epithelial carcinomas. The usually slow-growing and relatively nonaggressive carcinoid tumors had variable expression of TGF $\beta$ RII but were associated with the retention of mismatch repair protein function and a microsatellite-stable phenotype. *Cancer* 2005;103:229–36. © 2004 American Cancer Society.

**KEYWORDS:** carcinoid, microsatellite instability, mismatch repair, sequencing, transforming growth factor-beta receptor type II, tissue microarray.

**D**isruption of DNA mismatch repair genes that result in microsatellite instability (MSI) at simple repeated sequences plays an important role in human carcinogenesis by increasing the mutation rate of genes associated with cancer.<sup>1</sup> Two well characterized gene examples in which MSI has been identified include the growth regulatory receptor, transforming growth factor beta type II receptor

(TGF $\beta$ RII) and the mismatch repair protein, MSH2. Two microsatellite repeat regions have been found in the gene encoding TGF $\beta$ RII.<sup>2</sup> Mutation at the poly(A)<sub>10</sub> repeat sequence (BAT-RII) in the extracellular domain of TGF $\beta$ RII (with concomitant decreases in protein expression) is strongly correlated with the MSI phenotype and has been demonstrated in MSI-positive colon and gastric carcinomas.<sup>3-5</sup> Insertion of an extra GT into the coding poly(GT)<sub>3</sub> microsatellite region of TGF $\beta$ RII site also has been documented in colorectal and gastric carcinomas.<sup>2</sup> The BAT-26 region, a repeat of 26 deoxyadenosines located in intron 5 of *hMSH2*, is a highly accurate and sensitive indicator of MSI in colorectal and gastric carcinomas.<sup>4,6,7</sup>

Alterations in these regions are important because they have functional consequences. Loss of growth inhibitory response to TGF $\beta$  is considered to be an important step in the malignant progression of gastrointestinal (GI) tumors.<sup>8</sup> Frequent structural alterations of the TGF $\beta$ RII gene have been detected in human gastric carcinoma cell lines,<sup>9,10</sup> whereas colorectal carcinoma often exhibit mutations in BAT-RII, a phenomenon considered to engender a growth advantage to this tumor type.<sup>2</sup> It is noteworthy that inactivation of mismatch repair genes such as *hMLH1*<sup>11-14</sup> and *hMSH2*<sup>11-14</sup> has been observed in cancers with MSI or TGF $\beta$ RII gene mutations. Mutations in TGF $\beta$ RII may thus link DNA repair defects with a demonstrable pathophysiologic effect (i.e., an escape from growth regulation).<sup>2</sup>

In a preliminary study, we identified that a decrease in protein expression of TGF $\beta$ RII occurred in small bowel carcinoid tumors.<sup>15</sup> This suggested that growth inhibition via TGF $\beta$ RII activation was lost in these tumors. We postulated that mutations in TGF $\beta$ RII, perhaps due to MSI, resulted in a decreased TGF $\beta$ RII protein expression and the resultant aberrant growth-regulatory phenotype in small bowel carcinoid tumors. We examined protein staining of TGF $\beta$ RII on a carcinoid tumor tissue microarray to confirm that decreased TGF $\beta$ RII expression was associated with malignant disease (i.e., the development of lymph node and liver metastases). We then sequenced the poly(A)<sub>10</sub> and (GT)<sub>3</sub> regions in a series of small bowel carcinoid tumors that included localized and metastatic tumors. Thereafter, the region encompassing BAT-26 in the *hMSH2* gene was similarly analyzed. Alterations in mRNA levels of this gene as well as *hMLH1* were examined to assess whether these were present in small bowel carcinoid tumors, and protein staining of MSH2 was performed on a carcinoid tumor tissue microarray to evaluate the clinical significance of the expression of this mismatch repair protein.

## MATERIALS AND METHODS

### Tissue Specimens

Tumor tissue specimens were collected from 16 patients with histologically proven small bowel carcinoid tumors. The study was comprised of 11 males and 5 females with a median age of 55 years (range, 44–71 years). The patients had undergone resection of the primary tumor between 1997 and 2003 at the Yale University School of Medicine or were collected at the Cooperative Human Tissue Network (University of Pennsylvania, Pittsburgh, PA), which is funded by the National Cancer Institute. Primary tumors ( $n = 14$ ), liver metastases ( $n = 5$ ), and 1 lymph node from the 16 patients were studied. Paired normal tissue samples were also obtained from adjacent, macroscopically normal, nontumor mucosa in 6 patients.

### DNA Extraction

Genomic DNA was extracted from 26 freshly frozen tumor and normal tissue specimens from 16 patients using a QIAGEN DNeasy tissue kit (Qiagen, Valencia, CA).

### TGF $\beta$ RII [BAT-RII and (GT)<sub>3</sub> Repeat Sequences] Mutation Analysis

The BAT-RII repeat sequence and (GT)<sub>3</sub> microsatellite region of TGF $\beta$ RII were analyzed as previously described.<sup>2</sup> Briefly, DNA specimens from patients with small bowel carcinoid tumors were amplified by polymerase chain reaction (PCR) at two segments of TGF $\beta$ RII. The first segment was the poly-A region spanning nucleotides 621–794, which includes the (A)<sub>10</sub> microsatellite sequence in nucleotides 709–718. The second segment was the poly-GT region that extends from nucleotides 1908 to 2018 with a (GT)<sub>3</sub> microsatellite from 1931 to 1937.<sup>16</sup> The segments chosen were based on previous studies localizing most somatic TGF $\beta$ RII mutations to these loci in colorectal carcinoma cell lines and colorectal tumors.<sup>17</sup> Primers used to amplify the poly-A region were as follows: 5'-ACT AGA GAC AGT TTG CCA TGA-3' and 5'-ATA TTC TTC TGA GAA GAT GAT G-3'. For the GT region, 5'-ATG GTG TGT GAG ACG TTG ACT-3' and 5'-GCC GTC TTC AGG AAT CTT CT-3' were used. Conditions were comprised of 35 cycles at 94 °C for 1 minute, 50 °C for 1 minute, and 72 °C for 1 minute for the poly-A region, and 35 cycles at 94 °C for 1 minute, 56 °C for 1 minute, and 72 °C for 1 minute for the GT region. PCR reactions were performed in 25- $\mu$ L reaction volumes containing 0.2 mM of each dNTP, 1.5 mM (GT region), or 2.5 mM MgCl<sub>2</sub> (poly-A region), 1  $\times$  reaction buffer (Roche PCR core kit), 0.2  $\mu$ M of forward and reverse primer, 0.5 U Taq DNA Polymerase (Roche), and 100

**TABLE 1**  
**Characteristics of 55 Patients with Small Bowel Carcinoids on the Tissue Microarray**

Male:female ratio	Median age (yrs) (range)	Median tumor size (mm) (range)	Liver involvement	Lymph node involvement	Median follow-up (mos) (range)	Survival status ANED:AWD
28:27	62 (40–89)	15 (2–55)	12/41	21/31	43 (1–456)	10:45

ANED, Alive, no evidence of disease; AWD, alive with disease.

ng template DNA. PCR amplification products were excised and gel purified using the QIAquick gel purification kit (Qiagen) as per the manufacturer's instructions, and the products were eluted in 30  $\mu$ L of water. Purified PCR products were sequenced and analyzed by the W.M. Keck Biotechnology Resource Laboratory at Yale University using an automated Applied Biosystems 373A Stretch DNA sequencer (Perkin-Elmer, Norwalk, CT). PCR products were sequenced initially using the forward primer. If ambiguous peaks were present, then the sequence was confirmed with the reverse primer.

#### Microsatellite Instability Assays

Determination of MSI in small bowel carcinoid tumors was performed by sequence analysis of the BAT-26 locus, which is > 95% sensitive for detecting MSI.<sup>18</sup> The primers used for PCR amplification of this locus were 5'-TGA CTA CTT TTG ACT TCA GCC -3' and 5'-AAC CAT TCA ACA TTT TTA ACC C-3'. PCR reaction conditions were identical to those described for the poly-A region of TGF $\beta$ RII with the exception that 1.5 mM MgCl<sub>2</sub> was used in reactions. PCR products were purified and sequenced.

#### Quantitative Reverse Transcription-PCR

The *hMLH1* and *hMSH2* message was measured quantitatively as described<sup>19</sup> for seven tumors and five matched normal samples. Briefly, PCR was performed using the ABI 7900 Sequence Detection System (Applied Biosystems, Foster City, CA). The total RNA specimen from each sample was subjected to reverse transcription (RT) using the High Capacity cDNA Archive Kit (Applied Biosystems) following the manufacturer's suggestions. Briefly 2  $\mu$ g of total RNA sample in 50  $\mu$ L of water was mixed with 50  $\mu$ L of 2  $\times$  RT mix containing RT buffer, dNTPs, random primers, and multiscribe reverse transcriptase. The RT reaction was performed in a thermal cycler for 10 minutes at 25  $^{\circ}$ C followed by 120 minutes at 37  $^{\circ}$ C. Real-time PCR analysis was then performed in duplicate. Briefly, cDNA in 7.2  $\mu$ L of water was mixed with 0.8  $\mu$ L of 20  $\times$  assays on demand primer (*hMLH1* = Hs00179866, *hMSH2* = Hs00179887, glyceraldehyde-3-phosphate dehydro-

genase [GAPDH] = Hs99999905) and probe mix, 8  $\mu$ L of 2  $\times$  TAQMAN universal master mix in a 384-well optical reaction plate. The following PCR conditions were used: 50  $^{\circ}$ C for 2 minutes, then 95  $^{\circ}$ C for 10 minutes, followed by 40 cycles at 95  $^{\circ}$ C/0.15 minutes and 60  $^{\circ}$ C /1 minute. A standard curve was generated for each gene using cDNA obtained by pooling equal amounts from each sample ( $n = 12$ ). The expression level of the target genes was normalized to internal GAPDH. Data were analyzed using Microsoft Excel and calculated using the relative standard curve method (ABI, User Bulletin 2).

#### Tissue Microarray Immunostaining, Image Acquisition, and Data Analysis

Carcinoid tissue microarray slides containing 55 small bowel carcinoid tumor specimens (Table 1) that included the tumor ( $n = 16$ ) and normal tissue specimens ( $n = 6$ ) used for DNA studies were stained as described.<sup>20</sup> For antigen retrieval purpose, sections were immersed in citrate buffer (10 mM sodium citrate, pH 6.0) and subjected to 1  $\times$  10 minutes of high temperature/high pressure treatment followed by the treatment with 0.3% H<sub>2</sub>O<sub>2</sub> in methanol for 30 minutes at 37  $^{\circ}$ C to inactivate endogenous peroxidase. Slides were incubated for 24 hours at 4  $^{\circ}$ C with a 1:1000 dilution of the anti-TGF $\beta$ RII rabbit polyclonal antibody (Santa Cruz Biotechnology, Santa Cruz, CA) or with a 1:300 dilution of the anti-MSH2 protein mouse monoclonal antibody Ab-1 (Oncogene Research Products, Boston, MA). Goat anti-rabbit or anti-mouse antibodies conjugated to a horseradish peroxidase-decorated dextran polymer backbone (Envision; Dako, Carpinteria, CA) was used as a secondary reagent. For automated analysis, neuroendocrine tumor cells or normal mucosal epithelia were identified by the use of a fluorescently tagged anticytokeratin antibody cocktail (AE1/AE3; Dako), nuclei were visualized by 4', 6-diamidino-2-phenylindole (DAPI), and targets were visualized with a fluorescent chromogen (Cy-5-tyramide; NEN Life Science Products, Boston, MA).<sup>21</sup> Briefly, monochromatic, high-resolution (1024  $\times$  1024 pixel; 0.5  $\mu$ m) images were obtained of

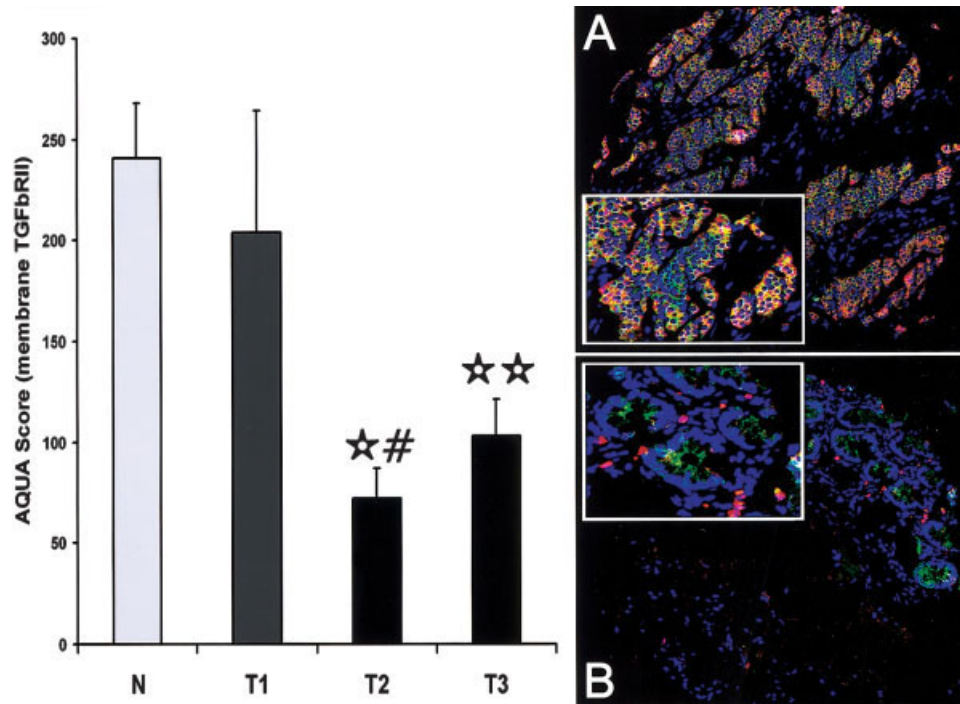


**FIGURE 1.** Automated quantitative analysis scores for transforming growth factor-beta type II receptor (TGF $\beta$ RII) protein expression in patients. Levels of membrane TGF $\beta$ RII were found to be significantly different between normal (white bar) mucosa and small bowel carcinoid tumor specimens (black bars) that developed lymph node metastases (T2) or liver and lymph node metastases (T3). No differences were observed between normal and tumor samples that did not develop metastases (T1). N: 55 normal samples; T: 55 primary tumor samples. Values are mean  $\pm$  the standard error of the mean. \* $P < 0.000001$  versus N. # $P < 0.05$  versus T1. \*\* $P < 0.0002$  versus N. Pseudo three-color images of two small bowel carcinoid tumor specimens are shown. Significant overlap is shown between cytokeratin and membrane TGF $\beta$ RII staining in the nonmetastatic tumor specimen (A: *inset*) but this finding was absent in the metastatic tumor specimen (B: *inset*). Immunostaining of TGF $\beta$ RII was invariably localized to the membrane. Blue: nuclei (4', 6-diamidino-2-phenylindole); green: tumor mask (cytokeratin–Alexa488); red: TGF $\beta$ RII (Cy5). Dual-membrane staining (red and green) results in yellow (Original magnification  $\times 100$ ).

each histospot. Areas of tumor or normal epithelia from stromal elements were distinguished by creating a mask from the cytokeratin signal. Coalescence of cytokeratin at the cell surface localized the cell membranes, and DAPI was used to identify nuclei. The TGF $\beta$ RII or MSH2 signal from the membrane or nuclear areas of tumor cells or epithelial cells was scored and expressed as signal intensity divided by the membrane area. Histospots containing  $< 10\%$  tumor, as assessed by mask area (automated), were excluded from further analysis. Previous studies have demonstrated that the staining from a single histospot provides a sufficiently representative sample for analysis.<sup>22</sup> Disc scores from the same tumor specimen were averaged to produce a single score. It has been determined previously that analysis of two cores concurs with the analysis of an entire tissue section with  $> 95\%$  accuracy.<sup>22</sup> The automated image acquisition and analysis using automated quantitative analysis (AQUA) is a set of algorithms developed by RLC at Yale University that allows for the rapid automated analysis of large-

scale cohorts of tumor samples on tissue microarrays. This generates reproducible continuous scale data that have the advantage over traditional pathology of discriminating subtle, low-level staining differences as well as being able to accurately score staining in subcellular compartments.

#### Statistical Analysis

Results were expressed as mean  $\pm$  the standard error of the mean and  $n$  indicates the numbers of patients in each study group. Statistical significance was calculated by the two-tailed Student  $t$  test for paired and unpaired values as appropriate, with a probability of  $P < 0.05$  representing statistical significance. The chi-square test was performed to evaluate the statistical significance of the two groups.

## RESULTS

### TGF $\beta$ RII Tissue Specimen Automated Quantitative Analysis Scores

An examination of TGF $\beta$ RII-stained histospots demonstrated that staining was invariably membrane

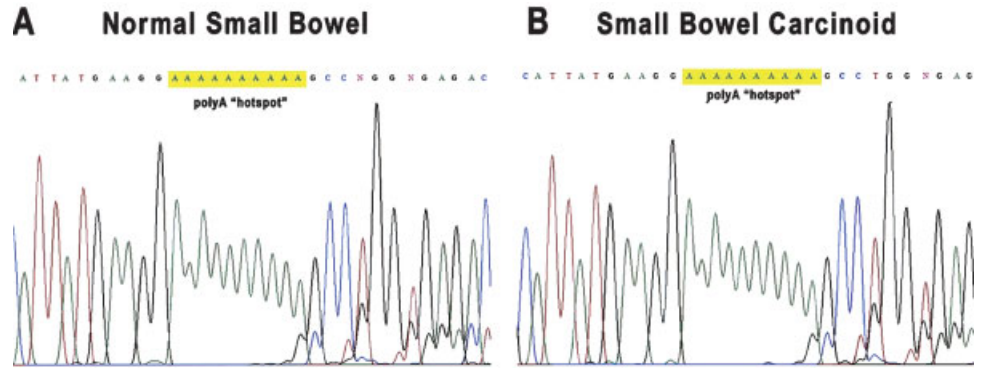


**FIGURE 2.** DNA sequences encompass the poly-A hotspot region (nucleotides 709–718) of the transforming growth factor-beta type II receptor gene. This 10-nucleotide region was conserved in (A) 6 normal small bowel mucosal samples and (B) 20 primary or metastatic small bowel carcinoid tumor specimens.

bound (Fig. 1), with AQUA expression levels ranging from 22 to 1099. Tumor specimens from patients who developed lymph node ( $n = 21$ ) or liver metastases ( $n = 12$ ) had significantly decreased TGF $\beta$ RII scores ( $P < 0.0002$ ) compared with normal mucosa specimens (Fig. 1). In addition, tumor specimens from patients who developed lymph node metastases ( $P < 0.05$ ) had significantly lower scores compared with patients with nonmetastatic tumors whereas lymph node metastatic tissue itself also demonstrated low receptor levels ( $P = 0.056$ ). Metastasis in small bowel carcinoid tumors is associated with a low protein expression of this inhibitory growth factor receptor.

#### TGF $\beta$ RII [BAT-RII and (GT) $_3$ Repeat Sequences] Mutation Analysis

Two repeat regions in the TGF $\beta$ RII gene were studied for mutations in 26 tumor and normal small bowel tissue samples. No frameshift mutations in the poly(A) $_{10}$  or (GT) $_3$  regions of TGF $\beta$ RII were detected in any of the carcinoid tumors (irrespective of metastasis), with normal and tumor samples sharing identical genotypes at these regions (Fig. 2). One frameshift mutation (an addition of A) in the poly(A) $_{10}$  of TGF $\beta$ RII was detected in one of three colorectal carcinoma samples (positive controls; data not shown).

#### Microsatellite Instability Assay

The BAT-26 poly-A tract within intron 5 of *hMSH2* either displayed 24, 25, or 26 adenine repeats in normal and tumor samples, which is congruent with the original description of this microsatellite as quasimonomorphic, with 1 major allele of 26 adenosine repeats and normal size variation not exceeding 2 nucleotides.<sup>23,24</sup> There was no association between tissue type and repeat number, and no shortening of size of the poly(A) $_{10}$  tract by 6–16 nucleotides in tumor DNA, a characteristic of the MSI phenotype.<sup>24,25</sup>

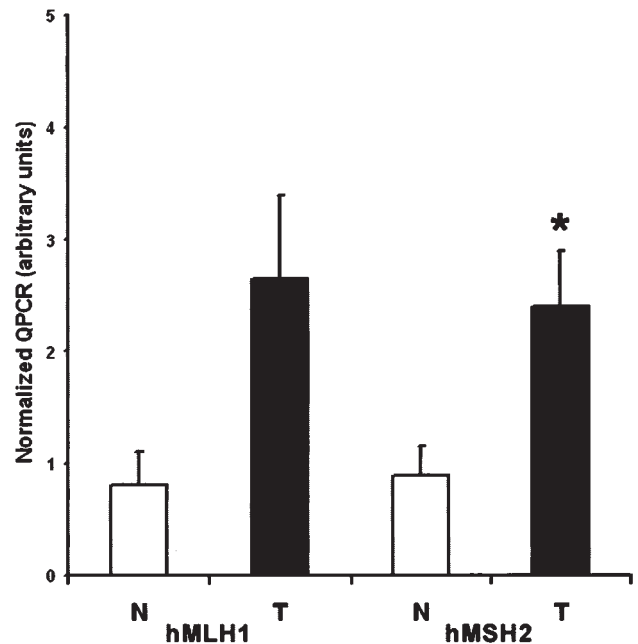


**FIGURE 3.** Message levels of *hMLH1* and *hMSH2* were determined by quantitative polymerase chain reaction (QPCR) in normal and tumor mucosal samples. QPCR values for *hMLH1* normalized to glyceraldehyde-3-phosphate dehydrogenase (GAPDH), although elevated, were not significantly altered ( $P = 0.06$ ). Levels of *hMSH2* were significantly increased in the group of tumor tissue samples compared with normal mucosal samples.  $*P < 0.05$ . Values are mean  $\pm$  the standard error of the mean. Black bars: seven tumor samples; white bars: five normal samples.

#### Quantitative RT-PCR

Although there was no statistically significant difference between *hMLH1* expression in tumor and normal samples, *hMSH2* mRNA levels were found to be significantly elevated in tumor samples compared with normal tissue samples (Fig. 3).

#### MSH2 Tissue Automated Quantitative Analysis Scores

An examination of MSH2-stained histospots demonstrated that staining was invariably nuclear (Fig. 4),

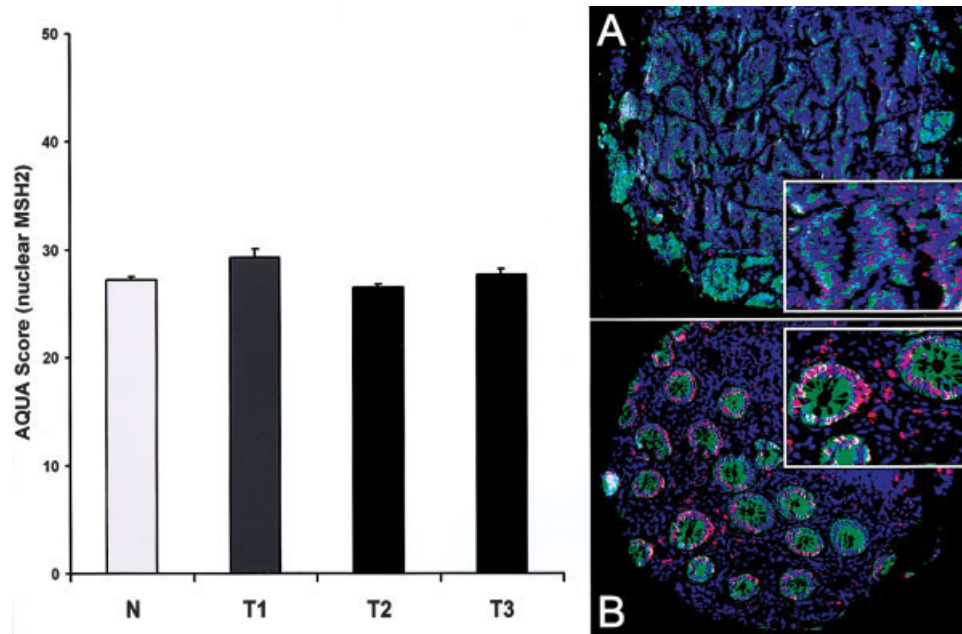


**FIGURE 4.** Automated quantitative analysis scores for MSH2 protein expression in patients. Levels of nuclear MSH2 were not significantly different between normal (white bars) mucosal samples and small bowel carcinoid tumors that were not metastatic (T1), or developed lymph node metastases (T2) or liver and lymph node metastases (T3) (black bars). N: 55 normal samples; T: 55 primary tumors. Values are mean  $\pm$  the standard error of the mean. Pseudo three-color images of a small bowel carcinoid tumor (A) and normal mucosa (B) Significant overlap is shown between cytokeratin and nuclear MSH2 staining in both the tumor and normal mucosa (*inset*). Immunostaining of MSH2 was invariably nuclear. Blue: nuclei (4', 6-diamidino-2-phenylindole); green: tumor mask (cytokeratin-Alexa488); red: MSH2 (Cy5). Dual nuclear staining (red and blue) results in purple. (Original magnification  $\times$  100.)

with AQUA expression levels ranging from 11 to 62. No differences in MSH2 protein levels were found between normal and small bowel carcinoid tissue samples irrespective of metastasis (Fig. 4).

## DISCUSSION

Mutation of the BAT-II microsatellite region of TGF $\beta$ RII is commonly observed in MSI colorectal tumors.<sup>2,4</sup> Mutations in this coding microsatellite region result in a truncated, nonfunctional TGF $\beta$ RII that has been shown to inactivate RII signaling and thereby facilitate tumorigenesis.<sup>2,3,17</sup> In the current study, antibody staining in a GI carcinoid tissue microarray demonstrated that TGF $\beta$ RII protein expression levels were variably expressed in small bowel carcinoid tumors. Primary tumors that did not metastasize had similar TGF $\beta$ RII levels to normal mucosa whereas metastatic (lymph node and liver) small bowel carcinoid tumors had significantly reduced TGF $\beta$ RII expression levels. Neither the BAT-II coding region nor the (GT)<sub>3</sub> microsatellite region within TGF $\beta$ II demonstrated molecular alterations between tumor and normal tissue samples. This absence of any mutations in the hotspot mutational regions of TGF $\beta$ RII indicates that abnormalities in transcriptional regulation or altered mRNA

stability or processing may be responsible for the decreased expression of TGF $\beta$ RII gene in small bowel carcinoid tumors. It is possible, but unlikely, that inactivating mutations in other portions of this gene not screened in the current study may be responsible for the reduction in expression of TGF $\beta$ RII in small bowel carcinoid tumors.

No evidence of MSI in small bowel carcinoid tumors in either the BAT-26 microsatellite locus in intron 5 of *hMSH2* or in the BAT-II microsatellite region of TGF $\beta$ RII was identified in the current study. Genetic abnormalities in chromosome 11 have been identified previously in carcinoid tumors.<sup>26</sup> That study also identified DNA mismatch repair gene mutations in  $>$  40% of these tumor specimens. The authors, however, could not categorically demonstrate MSI. In other studies, Ghimenti et al.<sup>27</sup> who examined 16 neuroendocrine tumors, including 3 small bowel carcinoid tumor specimens, using a panel of 6 microsatellite markers, and Arnold et al.<sup>28</sup> who examined 29 gastroenteropancreatic tumor specimens using 5 markers, found no evidence of MSI. The absence of MSI in small bowel carcinoid tumors identified in the current study is therefore a consistent feature of small bowel carcinoid tumors. It is interesting to note that

small bowel carcinomas exhibit MSI in approximately 20% of cases.<sup>29,30</sup> This suggests that epithelial tumors in this region of the gut probably develop similarly to colorectal tumors. In contrast, small bowel carcinoid tumors appear to evolve differently. The caveat to this interpretation is that although criteria have been developed for the identification of MSI in colon carcinoma due to hereditary nonpolyposis colorectal carcinoma, to our knowledge no gold standard exists for defining MSI in other conditions.<sup>31</sup>

Consistent with the absence of MSI in small bowel carcinoid tumors, *hMLH1* and *hMSH2* mRNA was not decreased in tumor samples. Expression levels of the *hMSH2* transcript were increased in tumor samples. This alteration, however, did not translate into a significantly elevated protein expression. AQUA of protein expression levels of MSH2 on the tissue microarray indicated no differences in levels between tumor and normal small bowel tissue samples. It is possible that the increased levels of the *hMSH2* transcript could reflect an increased protective effect in carcinoid tumors against mismatch-type mutational errors.

Genetic alterations reflecting mismatch repair do not occur in small bowel carcinoid tumors or their lymph node and liver metastases. The lack of mutations in TGF $\beta$ RII indicates that mechanisms other than protein truncation regulate the expression of this important growth-inhibitory regulator in these tumors. The molecular events leading to the formation of carcinoid tumors in the small bowel therefore are different to those resulting in epithelial carcinomas in the same organ. The indolent, slow-growing, and relatively nonaggressive nature of small bowel carcinoid tumors when compared with carcinomas of the GI tract may, perhaps, be explained by the retention of mismatch repair protein function and the microsatellite-stable phenotype of these carcinoid tumors despite alterations in TGF $\beta$ RII expression.

## REFERENCES

- Andrew SE, Peters AC. DNA instability and human disease. *Am J Pharmacogenomics*. 2001;1:21–28.
- Markowitz S, Wang J, Myeroff L, et al. Inactivation of the type II TGF-beta receptor in colon cancer cells with microsatellite instability. *Science*. 1995;268:1336–1338.
- Myeroff LL, Parsons R, Kim SJ, et al. A transforming growth factor beta receptor type II gene mutation common in colon and gastric but rare in endometrial cancers with microsatellite instability. *Cancer Res*. 1995;55:5545–5547.
- Parsons R, Myeroff LL, Liu B, et al. Microsatellite instability and mutations of the transforming growth factor beta type II receptor gene in colorectal cancer. *Cancer Res*. 1995;55:5548–5550.
- Oliveira C, Seruca R, Seixas M, et al. The clinicopathological features of gastric carcinomas with microsatellite instability may be mediated by mutations of different target genes—a study of the TGF $\beta$  RII, IGFII R and BAX genes. *Am J Pathol*. 1998;153:1211–1219.
- Wu MS, Lee CW, Sheu JC, et al. Alterations of BAT-26 identify a subset of gastric cancer with distinct clinicopathologic features and better postoperative prognosis. *Hepatogastroenterology*. 2002;49:285–289.
- Halling KC, Harper J, Moskaluk CA, et al. Origin of microsatellite instability in gastric cancer. *Am J Pathol*. 1999;155:205–211.
- Ijichi H, Ikenoue T, Kato N, et al. Systematic analysis of the TGF-beta-Smad signaling pathway in gastrointestinal cancer cells. *Biochem Biophys Res Commun*. 2001;289:350–357.
- Chang J, Park K, Bang YJ, et al. Expression of transforming growth factor beta type II receptor reduces tumorigenicity in human gastric cancer cells. *Cancer Res*. 1997;57:2856–2859.
- Park K, Kim SJ, Bang YJ, et al. Genetic changes in the transforming growth factor beta (TGF-beta) type II receptor gene in human gastric cancer cells: correlation with sensitivity to growth inhibition by TGF-beta. *Proc Natl Acad Sci USA*. 1994;91:8772–8776.
- Liu B, Nicolaidis NC, Markowitz S, et al. Mismatch repair gene defects in sporadic colorectal cancers with microsatellite instability. *Nat Genet*. 1995;9:48–55.
- Dietmaier W, Wallinger S, Bocker T, et al. Diagnostic microsatellite instability: definition and correlation with mismatch repair protein expression. *Cancer Res*. 1997;57:4749–4756.
- Macdonald GA, Greenson JK, Saito K, et al. Microsatellite instability and loss of heterozygosity at DNA mismatch repair gene loci occur during hepatic carcinogenesis. *Hepatology*. 1998;28:90–97.
- Nagai M, Kawarada Y, Watanabe M, et al. Analysis of microsatellite instability, TGF-beta type II receptor gene mutations and hMSH2 and hMLH1 allele losses in pancreaticobiliary maljunction-associated biliary tract tumours. *Anticancer Res*. 1999;19:1765–1768.
- Kidd M, Modlin IM, Lye KD, Hinoue T. The TGF beta-1 signaling pathway, mitogenic and fibrotic pathways in ileal carcinoids [abstract]. *Gastroenterology*. 2003;122:4(Suppl.):S1004.
- Furuta K, Misao S, Takahashi K, et al. Gene mutation of transforming growth factor beta1 type II receptor in hepatocellular carcinoma. *Int J Cancer*. 1999;81:851–853.
- Park K, Kin S-J, Bang Y-J, et al. Genetic changes in the transforming growth factor (TGF- $\beta$ ) type II receptor in human gastric cancer cells: correlation with sensitivity to growth inhibition by TGF- $\beta$ . *Proc Natl Acad Sci USA*. 1994;91:8772–8776.
- Myeroff LL, Parsons R, Kim SJ, et al. A transforming growth factor beta receptor type II gene mutation common in colon and gastric but rare in endometrial cancers with microsatellite instability. *Cancer Res*. 1995;55:5545–5547.
- Levenson A, Svoboda K, Pease K, et al. Gene expression profiles with activation of the estrogen receptor  $\alpha$ -selective estrogen receptor modulator complex in breast cancer cells expressing the wild-type estrogen receptor. *Cancer Res*. 2002;62:4419–4426.
- Camp R, Dolled-Filhart M, King B, Rimm D. Quantitative analysis of breast cancer tissue microarrays shows that both high and normal levels of Her2 expression are associated with poor outcome. *Cancer Res*. 2003;63:1445–1448.

21. Camp R, Chung G, Rimm D. Automated subcellular localization and quantification of protein expression in tissue microarrays. *Nat Med.* 2002;8:1323–1328.
22. Camp R, Charette L, Rimm D. Validation of tissue microarray technology in breast carcinoma. *Lab Invest.* 2000;80:1943–1949.
23. Hoang JM, Cottu PH, Benedicte T, et al. Bat-26, an indicator of the replication error phenotype in colorectal cancers and cell lines. *Cancer Res.* 1997;57:300–303.
24. Zhou XP, Hoang JM, Cottu P, Thomas G, Hamelin R. Allelic profiles of mononucleotide repeat microsatellites in control individuals and in colorectal tumors with and without replication errors. *Oncogene.* 1997;15:1713–1718.
25. Halling KC, Harper J, Moskaluk CA, et al. Origin of microsatellite instability in gastric cancer. *Am J Pathol.* 1999;155:205–211.
26. Jakobovitz O, Nass D, DeMarco L, et al. Carcinoid tumors frequently display genetic abnormalities involving chromosome 11. *J Clin Endocrinol Metab.* 1996;81:3164–3167.
27. Ghimenti C, Lonobile A, Campani D, Bevilacqua G, Caligo MA. Microsatellite instability and allelic losses in neuroendocrine tumors of the gastro-entero-pancreatic system. *Int J Oncol.* 1999;15:361–366.
28. Arnold CA, Sosnowski A, Blum HE. Analysis of molecular pathways in neuroendocrine cancers of the gastroentero-pancreatic system. *Ann N Y Acad Sci.* 2004;1014:218–219.
29. Muneyuki T, Watanabe M, Yamanaka M, et al. Combination analysis of genetic alterations and cell proliferation in small intestinal carcinomas. *Dig Dis Sci.* 2000;45:2022–2028.
30. Planck M, Ericson K, Piotrowska Z, et al. Microsatellite instability and expression of MKH1 and MSH2 in carcinomas of the small bowel. *Cancer.* 2003;97:1551–1557.
31. Boland CR, Thibodeau SN, Hamilton SR, et al. A National Cancer Institute workshop on microsatellite instability for cancer detection and familial predisposition: development of international criteria for the determination of microsatellite instability in colorectal cancer. *Cancer Res.* 1998;58:5248–5257.